Operation of a reversed pentacene-fullerene discrete heterojunction photovoltaic device

D. M. Nanditha, M. Dissanayake,[a] Ross A. Hatton, Richard J. Curry, and S. R. P. Silva
Nano-Electronics Centre, Advanced Technology Institute, University of Surrey, Guildford, Surrey GU2 7XH, United Kingdom

(Received 18 December 2006; accepted 8 February 2007; published online 12 March 2007)

The photoresponse of reversed bilayer organic photovoltaic device based on pentacene and C_{60} is examined, and the mechanism of photocurrent generation is shown to be different to that in conventional heterojunction devices, with free charge carriers generated at the electrode-organic interfaces rather than the organic heterojunction. This hypothesis is tested with silver nanoclusters incorporated at the organic heterojunction to quench excitons and facilitate recombination of free charge carriers, which shows a predicted increase in J_{sc}. The large V_{oc} in this reversed cell structure is also rationalized in the context of the model proposed. © *2007 American Institute of Physics*. [DOI: 10.1063/1.2713345]

The potential for low cost, flexible optoelectronic devices with large area capability has motivated significant research effort into the development of small conjugated organic molecule and polymer based light-emitting diodes (OLEDs) and photovoltaic devices (OPVs).[1] While the development of OLEDs has led to commercial products, OPVs have yet to show the performance required to enable their commercialization. OPVs are based on junctions between electron accepting and electron donating molecules, at which photoinduced excitons formed in both materials are dissociated to form free charge carriers. OPVs can be broadly categorized into two groups according to whether the photoactive component comprises two discrete layers of donor and acceptor molecules (bilayer) or a complex interpenetrating network (bulk heterojunction). To date, both bilayer and bulk-heterojunction OPVs have achieved power conversion efficiencies (η_p) of 4%–5% under 1 sun simulated solar illumination[2–5] which is considered to be half that required for market entry today. Furthermore, neither approach has a clear lead in the race to achieve commercial viability as yet.

To improve the performance of OPVs, the open circuit voltage (V_{oc}), short circuit current density (J_{sc}), and fill factor must all be optimized. Hence, it is essential to understand how these parameters relate to the fundamental physical processes of light absorption, exciton dissociation, charge carrier transport, and extraction to the external circuit. While the factors affecting V_{oc} are still the subject of debate,[6–9] it is generally accepted that the maximum attainable V_{oc} in heterojunction OPV is determined by the difference in potential between electrons in the lowest unoccupied molecular orbital (LUMO) of the acceptor material and the highest occupied molecular orbital (HOMO) of the donor material. Furthermore, the maximum V_{oc} is only achieved when photogenerated free charge carriers are extracted to the external circuit by the electrodes having Fermi levels aligned with these molecular orbital energies. Employing electrodes having a difference in work function greater than the donor HOMO–acceptor LUMO offset in an attempt to increase the built-in electric field is counterproductive, since free carriers have to surmount barriers to be extracted to the external circuit. The complexity of many metal-organic interfaces makes achieving optimal energy level alignment and predicting V_{oc} based on the work function of the pristine electrodes problematic.[10]

This letter reports the photoresponse of reversed discrete heterojunction OPV based on pentacene/C_{60} heterojunctions. To investigate the wider applicability of this study, reverse cell structures employing the soluble C_{60} derivative [6,6]-phenyl-C61 butyric acid methyl ester (PCBM) in place of C_{60} was also investigated and found to exhibit similar characteristics. Consequently, in the interests of conciseness, only the former is present herein with experimental results for the later included in the accompanying supplementary information.[11]

Twice sublimed pentacene (99.99%) was purchased from H.W. Sands. C_{60} (99.99%) and PCBM were purchased from American Dye Source and Solenne, respectively. All organic materials were used as received. Devices were fabricated on indium tin oxide (ITO) coated glass cleaned using a three stage ultrasonic bath treatment in toluene, an aqueous surfactant solution, and acetone. Immediately prior to use, the ITO substrates were suspended in the vapor of refluxing acetone followed by microwave oxygen plasma treatment. Discrete heterojunction OPVs were fabricated by subliming pentacene and C_{60} under high vacuum at a deposition rate of ~ 0.1 nm s^{-1} onto precleaned ITO glass substrates. Metal counterelectrodes to a 50 nm thickness were deposited at ~ 0.5 nm s^{-1} using a shadow mask without breaking vacuum. Current-voltage (J-V) measurements were performed using 100 mW cm^{-2} AM1.5 simulated solar irradiation.

The J-V characteristics of ITO/pentacene (45 nm)/C_{60} (50 nm)/Al (normal) and the ITO/C_{60} (50 nm)/pentacene (50 nm)/Al (reversed) devices are shown in Fig. 1. Figures 2(a) and 2(b) show the flatband energy level diagrams for both device configurations. The work functions of the clean ITO glass (Φ_{ITO}), measured directly using ultraviolet photoelectron spectroscopy, and the aluminium counter electrode (Φ_{Al}) were 4.4 (Ref. 12) and 4.3 eV, respectively. Notably, these schematic energy level diagrams do not account for the likely formation of abrupt vacuum level shifts, which often occur at metal-organic interfaces and which can drastically modify interfacial energy level alignment [Fig. 2(e)].[13] Remarkably, the J-V characteristics of both normal and reverse

[a]Electronic mail: m.dissanayake@surrey.ac.uk

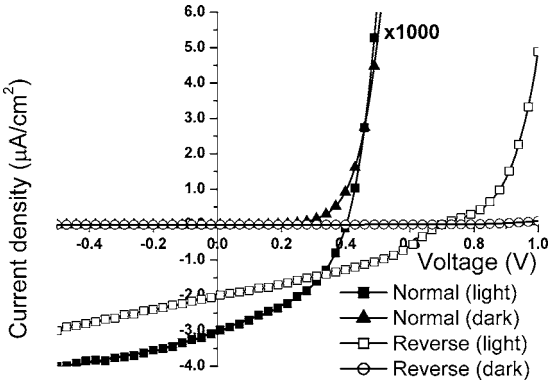

FIG. 1. *J-V* characteristics of ITO/pentacene/C_{60}/Al and ITO/C_{60}/pentacene/Al devices under dark and 100 mW cm^{-2} AM1.5 simulated solar irradiation conditions.

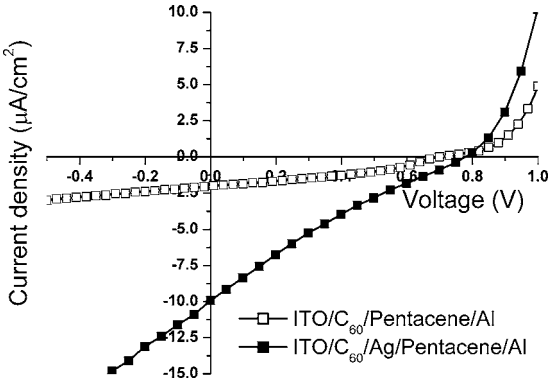

FIG. 3. *J-V* characteristics of ITO/C_{60}/pentacene/Al and ITO/C_{60}/Ag/pentacene/Al devices under 100 mW cm^{-2} AM1.5 simulated solar irradiation conditions.

devices biased relative to the ITO electrode have similar forth quadrant operation (Fig. 1), with Al and ITO accepting photogenerated electrons and holes, respectively. The V_{oc} of the normal cell structure (~0.4 V) is in good agreement with the difference in energy between the LUMO of C_{60} (4.5 eV) and HOMO of pentacene (4.9 eV),[14] consistent with the findings of Brabec *et al.* for bulk-heterojunction OPVs.[6] In order to rationalize the much larger V_{oc} in the reversed cell structure (~0.7 eV), it is necessary to consider the difference in energy between the HOMO of C_{60} (6.1 eV) and LUMO of pentacene (3.0 eV) since, based on the observed photoresponse (Fig. 1), electrons are extracted via the pentacene layer and holes via the C_{60} layer in the reversed cell structure. It is likely that the measured V_{oc} (~0.7 V) is much smaller than the maximum attainable V_{oc} (3.1 V) owing to nonideal alignment between the electrode Fermi levels and the relevant molecular orbitals in the adjacent organic layers. The fill factors in the normal and reverse device structures are comparable, being 0.43 and 0.38, respectively.

Figure 2(c) depicts the operation of the normal device.[15] Absorbed photons in the pentacene and C_{60} layers generate excitons which diffuse toward the donor-acceptor interface. At the interface, these excitons dissociate forming free electrons and holes in the acceptor (C_{60}) and donor (pentacene) layers, respectively. Free charge carriers drift toward the electrodes assisted by the built-in electrical field between the electrodes. This process of photocarrier generation forms the basis of operation of OPV and results in a relatively large J_{sc} (~3 mA cm^{-2}). However, this process cannot account for photocurrent generation in the reverse cell structure since the barriers to electrons and holes reaching the respective electrodes are prohibitively large (1.5 and 1.2 eV), respectively [Fig. 2(b)]. We propose the following explanation for the mechanism of photocurrent generation in the reverse cell structure schematically illustrated in Fig. 2(d): absorbed photons generate excitons in both the pentacene and C_{60} layers. Excitons generated in the pentacene layer are dissociated at the interface with the aluminium electrode, resulting in extraction of an electron to the external circuit and leaving a hole in the pentacene HOMO which is swept to the organic heterojunction by the built-in electric field. Excitons generated in the C_{60} layer are dissociated at the interface with ITO electrode resulting in extraction of a hole to the external circuit and leaving an electron in the C_{60} LUMO which is swept to the organic heterojunction by the built-in electric field. The resulting accumulation of both electrons and holes at the organic heterojunction is dissipated via recombination at the organic heterojunction.

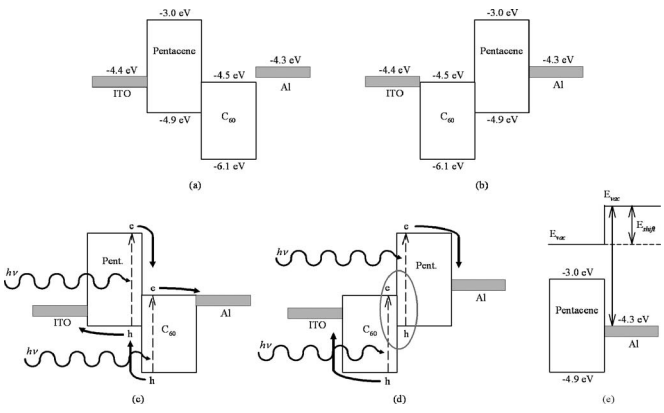

FIG. 2. Schematic flatband energy level diagrams for normal (a) and reverse (b) pentacene/C_{60} devices. Schematic operating principles for normal (c) and reverse (d) pentacene/C_{60} devices. (e) Example vacuum level shift at pentacene/Al interface.

To test the proposed mechanism, a 0.5 nm thick silver nanocluster layer was incorporated into the reverse cell structure by thermal evaporation at the pentacene-C_{60} interface to facilitate enhanced recombination of accumulated electrons and holes,[16] thereby increasing J_{sc}. The *J-V* characteristics of this cell (Fig. 3) exhibit a fivefold increase in the J_{sc} supporting the proposed mechanism of photocurrent generation. The shunt resistance of the reverse cell is reduced upon incorporation of Ag nanoclusters at the organic heterojunction owing to the increase susceptibility of these cell structures to filamentary shorting. Consequently, the fill factor is also reduced from 0.38 to 0.23. Furthermore, it is also clear from Fig. 3 that the cell series resistance is not significantly increased in the reverse cell structure despite the relatively low mobility of electrons in pentacene[17] and holes in C_{60}.[18] This is entirely consistent with the proposed mechanism of photocurrent generation since these low mobility carriers do not have to traverse the organic layers prior to extraction by the electrodes.

At first glance, the low J_{sc} in reversed cell structures indicates that the proposed mechanism of photogenerated carriers is inefficient as compared to the conventional mechanism of photocurrent generation at the organic heterojunction. However, it is likely that in the reverse cell structure, the process of free carrier generation at the organic hetero-

junction is still operative creating a reverse diffusion motivated current which counteracts the current generated via exciton dissociation at the organic-metal interfaces. Ag nanoclusters at the organic heterojunction act as recombination centers thereby reducing the efficiency, with which free carriers are generated via exciton dissociation at the organic heterojunction, consistent with the fivefold increase in J_{sc} upon incorporation of Ag nanoclusters. Furthermore, according to the proposed mechanism, the magnitude of J_{sc} in the reversed cell is ultimately limited by the requirement for balanced exciton formation and dissociation in the C_{60} and pentacene layers such that charge neutrality at the heterojunction is retained. Since the absorption coefficient of C_{60} (Ref. 19) is an order of magnitude below that of pentacene,[20] J_{sc} is expected to be limited by weak absorption in the C_{60} layer. The J_{sc}, in the reversed cell structure results in a power conversion efficiency of 0.0005%, which is three orders of magnitude lower than that of the normal device (0.52%).

There is also a significant "kink," near to zero field condition (V_{oc}), in the *J-V* characteristics of the reverse devices (Fig. 1). The physics behind the formation of such kinks is not thoroughly understood but is thought to relate to the effects of limitation in charge transfer between the active layer and the electrodes and due to interfacial recombination resulting in cycling of charges at the organic-electrode interfaces.[21] Interestingly, in the *J-V* characteristics of the reverse device with the Ag particles (Fig. 3), the kink is significantly reduced relative to the reference device. The removal of this kink can be attributed to the increase in the current as a result of improved charge extraction at the electrodes, which prevents accumulation of charges at the organic-electrode interface.

To conclude, in this letter we report the operation of reverse structure bilayer OPV. It is postulated that the mechanism of photocurrent generation in reverse cell structures is significantly different to that observed in normal heterojunction devices. The results presented indicate that charge carriers generated at the electrode-organic interfaces rather than at the organic heterojunction are the main contributor to the measured photocurrent. To test this hypothesis, we incorporated silver nanoclusters at the organic heterojunction to quench excitons and facilitate recombination of free charge carriers, resulting in a predicted increase of J_{sc}. The larger V_{oc} in these reversed cell structures can also be rationalized in the context of this model.

The authors wish to thank the EPSRC for a Portfolio Partnership award which has facilitated the research conducted in this project and the studentship awarded.

[1] S. E. Shaheen, D. S. Ginley, and G. E. Jabbour, MRS Bull. **30**, 10 (2005).
[2] S. E. Shaheen, C. J. Brabec, N. S. Sariciftci, F. Padinger, T. Fromherz, and J. C. Hummelen, Appl. Phys. Lett. **78**, 841 (2001).
[3] P. Peumans and S. R. Forrest, Appl. Phys. Lett. **79**, 126 (2001).
[4] J. G. Xue, S. Uchida, B. P. Rand, and S. R. Forrest, Appl. Phys. Lett. **85**, 5757 (2004).
[5] G. Li, V. Shrotriya, J. S. Huang, Y. Yao, T. Moriarty, K. Emery, and Y. Yang, Nat. Mater. **4**, 864 (2005).
[6] C. J. Brabec, A. Cravino, D. Meissner, N. S. Sariciftci, T. Fromherz, M. T. Rispens, L. Shanchez, and J. C. Hummelen, Adv. Funct. Mater. **11**, 374 (2001).
[7] A. G. Umnov and O. J. Korovyanko, Appl. Phys. Lett. **87**, 113506 (2004).
[8] A. Gadisa, M. Svensson, M. Anderson, and O. Inganas, Appl. Phys. Lett. **84**, 1609 (2004).
[9] J. Nelson and J. Kirkpatrick, Appl. Phys. A: Mater. Sci. Process. **A79**, 15 (2004).
[10] A. Moliton and J. Nunzi, Polym. Int. **55**, 583 (2006).
[11] See EPAPS Document No. E-APPLAB-90-103710 for *J-V* characteristics of pentance/PCBM discrete heterojunction normal and reversed OPVs and absorption measurements of pentacene and C_{60}. This document can be reached via a direct link in the online article's HTML reference section or via the EPAPS homepage (http://www.aip.org/pubservs/epaps.html).
[12] A. J. Miller, R. A. Hatton, and S. R. P. Silva, Appl. Phys. Lett. **89**, 123115 (2006).
[13] H. Ishii, K. Sugiyama, E. Ito, and K. Seki, Adv. Mater. (Weinheim, Ger.) **11**, 605 (1999).
[14] S. Yoo, B. Domercq, and B. Kippelen, Appl. Phys. Lett. **85**, 5427 (2004).
[15] P. Peumans, A. Yakimov, and S. R. Forrest, J. Appl. Phys. **93**, 3693 (2003).
[16] Jiangeng Xue, Soichi Uchida, Barry P. Rand, and Stephen R. Forrest, Appl. Phys. Lett. **85**, 5757 (2004).
[17] K. N. Narayanan Unni, Ajay K. Pandey, Salima Alem, and Jean-Michel Nunzi, Chem. Phys. Lett. **421**, 554 (2006).
[18] R. Könenkamp, G. Priebe, and B. Pietzak, Phys. Rev. B **60**, 11804 (1999).
[19] A. P. Moravsky, P. V. Fursikov, N. V. Kiryakov, and A. G. Ryabenko, Mol. Mater. **7**, 241 (1996).
[20] J. Puigdollers, C. Voz, A. Orpella, I. Martin, M. Vetter, and R. Alcubilla, Thin Solid Films **427**, 367 (2003).
[21] J. Nelson, J. Kirkpatrick, and P. Ravirajan, Phys. Rev. B **69**, 035337 (2004).